Original Paper Open Access

Root response to temperature extremes: association mapping of temperate maize (*Zea mays* L)

Regina Reimer[1], Benjamin Stich[2], Albrecht E Melchinger[3], Tobias A Schrag[3], Anker P Sørensen[4], Peter Stamp[1], Andreas Hund[1]*

[1]ETH Zurich, Institute of Plant, Animal and Agroecosystem Sciences, 8092 Zurich, Switzerland
[2]Max Planck Institute for Plant Breeding Research, 50829 Cologne, Germany
[3]Institute for Plant Breeding, Seed Science and Population Genetics, University of Hohenheim, 70593 Stuttgart, Germany
[4]Keygene NV, PO.Box 216, 6700 AE Wageningen, The Netherlands
*Corresponding author: E-mail: andreas.hund@ipw.agrl.ethz.ch

Abstract

Little is known about the genetic control of the root architecture of maize (*Zea mays* L) and its response to temperature extremes. An association mapping panel, including 32 flint and 42 dent inbred lines, was characterized for root traits. The growth of axile and lateral roots was assessed non-destructively in growth pouches at 16°C (chilling), 28°C (control) and 36°C (heat). Association mapping was done using the PK_{Opt} mixed-model association-mapping approach. Heat slowed down the development of seedling roots to a lesser extent than chilling, but differences between the heterotic groups were observed mainly at optimal temperature. Of 1,415 AFLP markers, 70 showed significant marker-trait associations and 90 showed significant marker-trait associations with temperature interaction effects. Compared to the flint lines, the dents showed stronger growth of axile roots, especially under optimal conditions, and carried more of the trait-increasing alleles for the length of axile roots. In contrast, the flints accumulated more root dry weight at low temperature and exclusively carried the alleles favoring tolerance to chilling. A combination of inbreds carrying alleles positive for performance under contrasting temperature conditions should lead to a complementary effect in the hybrid and would increase adaptation to a wider range of temperature.

Keywords: corn, root growth, cold, heat, QTL

Abbreviations: k_{Lat} - Relative elongation rate of lateral roots; ER_{Ax} - Elongation rate of axile roots; k_{Lat}/ER_{Ax} - Ratio of lateral to axile root elongation rate

Expressions used: associations with temperature treatment interaction effects = marker-by-temperature interaction

Introduction

The adaptation of maize to a wide range of environmental conditions including temperature remains a central target of breeding programs. Maize breeders work with inbred lines that are selected for their ability to produce superior, well adapted commercial hybrids. Temperate hybrids in northern and central Europe are usually a cross of inbred lines from the heterotic groups flint and dent (Shaw, 1988). Both were established in the 1950s, based on European flint landraces and lines of Corn Belt Dent. The flint lines contributed chilling tolerance and the dent lines contributed a high yield potential (Hallauer, 1990). It may be speculated that in the past 60 years breeders improved chilling tolerance in both heterotic groups but little research has been done to evaluate if this was really the case.

In cool temperate climates maize is sown as early as possible when soil temperatures are above 7 to 8°C to ensure a high and consistent yield. However, when temperatures are low for a prolonged period of time they have severe negative effects on early development. Chilling decreases the photosynthetic performance of maize seedlings (Fracheboud et al, 1999) as well as the root growth and leaf expansion (Engels, 1994; Hund et al, 2008; Stone et al, 1999). There is not much information how heat stress affect root growth in maize but tropical maize inbred lines differ with respect to the sensitivity of their axile roots to high temperatures (Trachsel et al, 2010a). Temperate maize is rarely affected by high temperature during the seedling stage but maize selected for the coldest areas of northern Europe is known to suffer frequently from heat stress during later stages (Frei, 2000).

Early maize hybrids are considered to be a potential second-season crop when winter barley may be harvested earlier in southern regions of central Europe. Accordingly, seedlings may be exposed to chilling stress when sown in spring or to heat stress when sown in summer. A range of physiological and morphological adaptation is required to achieve ad-

 RECEIVED 03/17/2013

aptation to chilling and heat stress. Physiological adaptation to heat and chilling includes activation of the antioxidant system and the accumulation of soluble carbohydrates. Antioxidants prevent damage to the plant caused by reactive oxygen species (Nietosotelo and Ho, 1986; Timperio et al, 2008). Furthermore, morphological adaptation may be beneficial to plant productivity, for example through the development of more lateral roots (Hund et al, 2008) or an increase in root diameter (Cutforth et al, 1986) at low temperature. Adaptation mechanism of plants to heat and cold may follow either common response pathways or temperature-specific pathways. Furthermore, adaptation mechanisms to cold or heat may have adverse negative effect under the respective opposite temperature stress. The rapid accumulation of antioxidants or soluble carbohydrates is an example for a similar response, which is required under heat and chilling stress. By observing the allele effects that underlie the response to temperature extremes, the reaction type becomes evident. So far, little effort has been made to trace the effect of an allele over the whole range of temperatures, to which a maize plant may be exposed, depending on the environment and developmental stage. There is evidence that inbred lines differ with respect to their temperature optima leading either to greater heat or to greater chilling tolerance. Furthermore, the combination of relatively chilling sensitive inbred lines, with a lower temperature optimum, and relatively heat tolerant inbred lines, with a higher temperature optimum, leads to hybrids combining both parental characteristics, chilling and heat tolerance (Hund et al, 2012). This combination of both, heat and chilling tolerance in hybrids may be explained by concept of 'marginal overdominance' in which the hybrid, summed over all situations, expresses higher relative fitness than its parents (Wallace, 2000).

Yet little is known about the genetic architecture of temperature tolerance of breeding populations used for hybrid maize breeding and there is almost no information about QTLs affecting temperature responses of root growth.

Quantitative trait loci of maize were identified for root traits in relation to early vigor (Hund et al, 2004) as well as for physiological traits and growth under chilling stress (Jompuk et al, 2005). More information exists for seedling root traits at optimal temperature (Hund et al, 2004; Ruta et al, 2010; Trachsel et al, 2009; Tuberosa et al, 2003). All these QTL studies were based on biparental crosses, which have the disadvantage of being limited by the number and the resolution of alleles that can be sampled. Alternatively, in the mapping of marker-trait associations in plant-breeding populations, a high number of alleles can be mapped simultaneously at a high resolution (Flint-Garcia et al, 2003). Statistical methods, to account for population structure minimize the risk of false-positive associations (Pritchard et al, 2000) but may also increase the risk to underestimate the effect of alleles that are confounded with population structure, as shown, for example, for the D8 allele conferring earliness (Camus-Kulandaivelu et al, 2006).

We are not aware of any QTL mapping or phenotyping of root growth in the flint-by-dent heterotic pattern. Our primary goal was to evaluate the groups for differences with regard to the response of root growth to low and high temperatures. We chose to screen a comparably large set of 74 genotypes which allowed not only for a sound phenotypic characterization of the heterotic groups, but also for a genome-wide association mapping. Our second objective was to identify putative key loci. We used the putative alleles at these loci to elucidate their type of response, i.e. if they were involved in tolerance to chilling, heat or both, and the degree to which the alleles were fixed within either pool. The degree of fixation was used as indicator for the degree to which the pools are separated with respect to these loci either due to ancient population structure or selection.

Materials and Methods

We used a set of 74 European maize inbreds of flint (32) and dent (42) lines from a breeding program at the University of Hohenheim. Seeds from all genotypes used in this study were from one seed batch and, thus, are expected to contain similar levels of seed nutrients. Information about population structure and linkage disequilibrium of this germplasm has been described elsewhere (Stich et al 2005; 2006). In short, LD was significant ($p < 0.05$) for about 15% of the AFLP marker pairs and for about 49% of the SSR marker pairs in each of the two germplasm groups, flint and dent. In both germplasm groups, the ratio of linked to unlinked loci pairs in LD was higher for AFLPs than for SSRs. The LD blocks between SSR markers were on average 30 cM. The LD blocks between AFLPs were about 4cM shorter than those between SSR markers. The observation of LD due to linkage for both marker types suggested that genome-wide association mapping should be possible using either AFLPs or SSRs.

Plant growth

Plants were tested under chilling stress (16°C), close-to-optimal temperature (28°C) and mild heat stress (36°C). The upper and lower temperatures are considered to be temperature extremes. These temperatures were based on preliminary studies of a wide range of favorable and unfavorable conditions. Roots stopped growing at 15°C and 40°C and grew best at 28°C (Hund et al, 2012).

Seeds were imbibed over night at room temperature, surface sterilised with 2.5% sodiumhypoclorite-solution (NaOCl (aq)) for 10 min, rinsed thoroughly with distilled water, and germinated on filter papers (Ø 70 mm, Macherey-Nagel AG, Oensingen, Switzerland) in an incubator at 27 °C. Seedlings with a similar radicle

length were transferred to growth pouches (Hund et al, 2009) and cultivated until the respective V2 stage, indicated by a fully visible collar on the second leaf. The pouches were made of black plastic sheeting and contained blue germination blotting paper (24 × 29.5 cm; Anchor Paper, St. Paul, MI, USA) and were hung in growth containers (33 cm wide × 132 cm long × 33 cm high). The bottom of the pouch was submerged in nutrient solution (0.23% (v/v) of Wuxal®, Aglukon Spezialdünger GmbH, Düsseldorf, Germany; composition per liter: 100 g N, 100 g P_2O_5, 75 g K_2O, 190 mg Fe, 162 mg Mn, 102 mg B, 81 mg Cu, 61 mg Zn, 10 mg Mo). To establish the seedlings, they were grown under optimal conditions (28°C) for two days. The photoperiod throughout the experiment was 12 h, the photosynthetic photon flux density (PPFD) was 350 µmol m^{-2} sec^{-1} and the relative humidity 60%. The temperature treatments were commenced two days after transplanting the seedlings, when lateral roots had appeared. At harvest, the roots were carefully removed from the blotting paper. The root material was dried at 60°C to constant weight and the dry matter determined.

Imaging and analyses

Images were taken at three specified times by a flatbed scanner (HP scanjet 4600 series, 'see-through', Hewlett-Packard Company): i) before the application of the temperature treatment (t_0) to determine the initial root length, ii) halfway through the treatment period (t_1) to determine the increase of root length as a function of time and iii) at the V2 stage when the plants were harvested (t_2) to determine root morphology depending on the stage. To scan the roots, the pouch was placed on a specially built rack. The front of the pouch was opened and the pouch was fixed; the scanner was in a horizontal position in front of the blotting paper. The acquired 24 bit images were subsequently processed by Adobe Photoshop 7.0 in three steps (Adobe Systems Inc, San Jose, CA, USA). First, the saturation channel was used to obtain 8-bit images with enhanced contrast between roots and the background. Second, the median filter with a radius of three pixels was used to remove noise, which may have been present when detecting spurious roots by WinRHIZO 2003b (Regent instruments, Montreal, QC, Canada). Third, binary images were obtained by applying a threshold to the tonal value. These images were manually controlled to ensure quality of the data, which was subsequently processed by WinRHIZO, revealing 72 width classes (diameter for roots) ranging from 42.33 µm (1 pixel) to 3.05 mm (72 pixels). The debris removal filter was set to remove objects with an area smaller than 0.02 cm2 and a length/width ratio lower than 5. Axile roots of maize form the major structure of the root system and usually have diameter above 0.8 mm. Their lateral roots usually have diameters below that threshold and explore the soil at short distance (Hund et al, 2009; McCully, 1999). By using their root diameter as choice criterion the lengths of axile and lateral roots were extracted from the root length in diameter-class distribution (RLDD) obtained by WinRHIZO as described by Hund et al (2009). Accordingly, the length of axile or lateral roots determined by image processing includes all three root types, i.e. the primary, seminal and crown roots. However, root diameters depend on environmental factors such as temperature. Accordingly, axile and lateral roots were separated by temperature-dependent thresholds determined by evaluating the bimodal shape of the RLDD (See Hund et al, 2009) for each temperature.

The elongation rate of the axile roots (ER_{Ax}) was linearly modeled, and the elongation rate of the lateral roots (k_{Lat}) was exponentially modeled (Hund et al, 2009; Ruta et al, 2009). The corresponding models were

$$x(t) = x(t_0)ER_{Ax}t; \quad ER_{Ax} = \frac{x(t) - x(t_0)}{t} \qquad (1)$$

for axile root elongation, where x(t) is the root length at time t after germination, x(t0) is the root length at the first scanning day, and Δt is the lag between t and t_0 and

$$x(t) = x(t_0)e^{k_{lat}t}; \quad k_{lat} = \frac{\log(x(t) - x(t_0))}{t} \qquad (2)$$

for lateral root elongation rate, where klat is the growth constant for lateral roots. The growth constant k is inversely proportional to the doubling time of the length of lateral roots.

In addition to image processing, the numbers seminal roots (i.e. the number of roots emerging from the scutellar node) were counted. All roots are termed and abbreviated according to the terminology described by Hund et al (2011).

Experimental design and statistics

The experimental design within each temperature environment (t_j) was an alpha lattice design (Barreto et al, 1997) with eight biological replications, i.e. four independent growth chamber replications per environment (r_{jk}) and two blocks (b_{jkl}) per growth chamber, each containing a full set of inbred lines ($\breve{g}_i$). The 74 inbred lines in each block were distributed across eight incomplete blocks (c_{iklm}), which were distributed in four sections in each of two growth containers. The final model to obtain the best linear unbiased estimates (BLUEs) of genotypes was:

$$Y_{ijklm} = \mu + \breve{g}_i + t_j + \breve{g}t_{ij} \mid \breve{g}tr_{ijk} + r_{jk} + b_{jkl} + c_{jklm} + e_{ijklm} \quad (3)$$

where Y_{ijklm} is the effect of the i^{th} inbred line in the j^{th} environment, the k^{th} growth chamber run, the l^{th} block and the mth growth container. e_{ijklm} is the residual error and µ the intercept. The terms to the left and right of the vertical line (|) are considered to be fixed and random, respectively. Analysis of variance was done using the asreml-R package (ASReml release 2.0, Gilmour et al, 2006) and the best linear unbiased estimates (BLUEs), extracted for each genotype-by-

treatment combination, were the input values for the association mapping.

The analysis of variance of the heterotic groups, flint and dent, and for the heterotic group-by-environment interaction was made according to the final model:

$$Y_{ijklmn} = \mu + t_j + h_n + th_{jn} \mid \breve{g}_i + \breve{g}t_{ij} + \breve{g}tr_{ijk} + r_{jk} + b_{jkl} + c_{jklm} + e_{ijklmn} \quad (4)$$

where Y_{ijklmn} is the effect of the ith inbred line in the nth heterotic group, in the jth environment, the kth growth chamber run, the lth block and the mth container. h is the nth heterotic group (flint or dent); all other parameters are the same as in model 3. If not stated, then the effects of the extreme temperatures on traits are given in comparison to close-to-optimum temperature.

The heritability based on an entry means (Holland et al, 2003) for each treatment was calculated as:

$$h^2 = \frac{\sigma^2_{\breve{g}}}{\sigma^2_{\breve{g}} + \frac{1}{j}\sigma^2_{\breve{g}t} + \frac{1}{jk}\sigma^2_{\breve{g}tr} + \frac{1}{jkl}\sigma^2_r} \quad (5)$$

where $\sigma^2_{\breve{g}}$ is the genetic variance, $\sigma^2_{\breve{g}t}$ the variance of the genotype-by-temperature interaction, the variance of the genotype-by-temperature-by-run interaction, and σ^2_r the residual error variance. j, k, and l denote the number of treatments (3), runs (4), and blocks (2), respectively. $\sigma^2_{\breve{g}}$ is the genetic variance after correction for effects of the heterotic group.

Association mapping

We conducted genome-wide association mapping of 74 maize inbred lines, genotyped with 1415 AFLPs, of which 748 were mapped to one of the 10 chromosomes on the Keygene integrated map (unpublished). The remaining markers are mapped to pseudo chromosomes. First, we analyzed the population structure of the lines. Second, the main marker effects and marker-by-temperature interaction effects were determined for the seedling growth traits. To detect markers linked to genome regions associated with a specific stress response, markers showing significant interactions with the environment were classified according to their allele substitution effects. Finally, we attempted to shed light on the distribution of alleles, which increase tolerance in the heterotic groups.

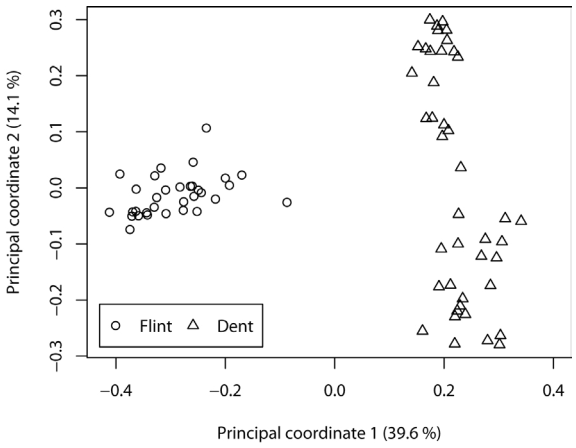

Figure 1 - Principal coordinate analysis based on Rogers' distance estimates. Flint lines (open circles) dent lines (triangles).

Analysis of population structure

This analysis was performed based on 163 SSRs (Schrag et al, 2010) using the R Statistics Software (R Development Core Team, 2008). The Rogers' distance (RD) was calculated according to Rogers (1972). Associations among the 74 inbred lines were revealed by a principal coordinate analysis (Gower, 1966) based on RD estimates between pairs of inbreds. Analysis of the first principal coordinate (PC1) explaining 39.6% of the variance revealed a clear separation of the heterotic groups, flint and dent, confirming that they are two distinct groups (Figure 1).

The combined analysis of adjusted entry means (BLUEs) across environments, obtained from model (3), did not enable us to infer entry-by-environment interactions (cf. Piepho, 2000). Nevertheless, the results of Stich et al (2008a) indicate that the power for detection of marker-phenotype associations with a two-step approach based on adjusted entry means for each environment is only slightly lower than with a one-step approach. Therefore, our analyses were based on adjusted entry means for each environment.

The PKopt method described by Stich et al (2008b) was used to detect AFLP phenotype associations:

$$M_{ijp} = \mu + \sum_{u=1}^{z} P_{iu} v_u + l_j + a_p + (al)_{jp} + \breve{g}_i + e_{ijp} \quad (6)$$

where M_{ijp} is the adjusted entry mean of the ith maize inbred in the jth environment carrying the pth allele, μ is the intercept, v_u the effect of the uth column of the population structure matrix **P**, l_j the effect of the jth environment, a_p the effect of allele p, $(al)_{jp}$ the interaction effect of the pth allele with the jth environment, $\breve{g}_i$ the genetic effect of the ith entry except for a_p, and e_{ijp} the residual.

According to Zhao et al (2007), the first two principal components (z = 2) of the SSR allele frequency matrix, which explained 53.7 % of the variance (c.f. Figure 1), were used as the **P** matrix. The variance of the random effects $\breve{g} = \breve{g}_1,...,\breve{g}_{74}$ and e = (e1, 1, 1,..., e74, 3, 2) was assumed to be Var($\breve{g}$) = $2\mathbf{K}_{opt}\sigma^2_{\breve{g}}$ and Var(e) = $\mathbf{R}\sigma^2_r$, where $\mathbf{K}_{opt}$ is a 74×74 matrix of kinship coefficients, defining the degree of genetic covariance between all pairs of entries, and **R** 222 × 222 the identity matrix. Genetic variance, $\sigma^2_{\breve{g}}$ and residual variance, σ^2_r were both estimated by REML. For each examined trait, $\mathbf{K}_{opt}$ was calculated according to Stich et al (2008b) using the SSR markers.

To solve the multiple test problem, the Bonferroni-Holm procedure (Holm, 1979) was applied to detect AFLPs with significant (P < 0.05) 1) main effects across environments; and 2) AFLP × environment interactions. The proportion of genotypic variance, explained by one marker, was calculated from the reduction of the genetic variance in a model with marker effects compared to the genetic variance in a model without marker effects. The total proportion of genotypic variance explained by all AFLPs with significant main effects was obtained by fitting a model, which included all markers. All mixed-model calculations were performed with the ASReml release 2.0 (Gilmour et al, 2006).

Test for group specificity

We determined whether the detected associations were partly associated with the heterotic group. Thus, the frequency of alleles in the flint group was assessed for trait-associated markers. The frequency was expressed as the ratio of the number of flints carrying the allele to the total number of genotypes carrying the allele. This ratio flint (c.f. Supplementary Table 1) was 0 when the allele was absent in the flint group, and was 1 when the allele was detected in the flints but not in the dents. A χ^2 two sample test was conducted to determine whether the heterotic groups differed in the frequency of alleles, i.e. whether the alleles were group-specific. The average effect of the flints (Effect flint, Supplementary Table 1 and 2) on the traits of a virtual flint-by-dent hybrid was qualified based on the allele substitution effect and the frequency of alleles in the flint pool. In the case of the loci with association-by-temperature interactions, the "effect flint" revealed the relative change in the allele effect at temperature extremes compared to the control. For example, a positive "effect flint" was found when α½ changed positively from the optimum to the extreme and the trait-increasing allele was more frequent in the flints (Supplementary Table 1).

The detected associations were projected on the IBM2 2008 Neighbors Frame (Schaeffer et al, 2008) genetic map (called Neighbors 2008 in the following), obtained from the Maize Genetics and Genomics Database (MaizeGDB, Lawrence et al, 2005) by the BioMercator software (Arcade et al, 2004) using 135 common SSR markers. Association clusters were assigned when multiple associations for the same trait were detected on the same chromosome within a region of ±20 cM on Neighbors 2008. The respective number of detected associations is given in parentheses (Figure 2). Collocation of marker-trait associations of different traits was considered to be positive when the α1/2 had the same algebraic sign (+ or –) and negative when the signs were opposite. Temperature-tolerance genes in the ± 20 cM region around the detected associations were selected from the Neighbors 2008 map to pinpoint the most interesting associations.

Classification of allele responses

The allele substitution effect (α1/2) is given as the additive effect of replacing allele 1 by allele 2. To obtain the relative allele substitution effects, we set the absolute α1/2 relative to the adjusted means (BLUEs). Figure 3 shows the allele responses to temperature. Allele-by-temperature treatment interaction effects are shown for close-to-optimal (here 28°C) and extreme (here 16°C and 36°C) temperature. Allele 2 (A2) shows two possible reactions of one allele in relation to the reference allele 1 (A1). The allele confers tolerance to only one of the temperature extremes (a), both temperature extremes (b), or indifferent (c). Classes are subdivided into those with crossover interactions

Table 1 - Adjusted means for population and heterotic groups (flint and dent) within temperature treatments for various measured traits. For explanation of the acronyms in the table header, see Table 2. Proportion of total variance of genotype (G), genotype-by-treatment interactions (G×T) and genotype-by-treatment-by-run interactions (G×T×R) as well as heritability estimates ($\mathbf{h}^2$). ANOVA results for the effect of treatment (T) heterotic group (HetGr) and their interaction.

		ER_{Ax} cm d^{-1}	k_{Lat} d^{-1}	L_{Ax} cm	D_{Ax} mm	SA_{Ax} cm^2	L_{Lat} cm	D_{Lat} mm	SA_{Lat} cm^2	No_{Se}	DW_{Rt} mg	DW_{RSt} mg mg^{-1}	SA_{Rt} cm^2	L_{Rt} cm	k_{Lat}/ER_{Ax}
Population mean															
16 °C		2.62	0.123	57.6	1.00	192	22.8	0.317	23.1	1.78	43.3	0.750	219	81.4	0.072
28 °C		9.35	0.641	56.9	0.85	160	19.1	0.250	15.1	1.70	33.3	0.628	180	75.3	0.090
36 °C		6.55	0.436	57.4	0.94	176	25.7	0.306	24.9	1.81	32.1	0.599	206	85.3	0.087
Heterotic Group															
16 °C	flint	2.39	0.122	52.7	1.043	183	22.0	0.316	22.4	1.60	44.3	0.779	211	76.0	0.074
	dent	2.68	0.124	60.3	0.965	195	21.7	0.318	22.2	1.91	41.4	0.700	221	82.1	0.071
28 °C	flint	8.16	0.664	50.5	0.890	149	17.7	0.253	14.0	1.55	31.7	0.629	169	66.8	0.097
	dent	10.08	0.611	60.7	0.812	164	19.1	0.246	15.1	1.80	34.0	0.604	184	78.5	0.084
36 °C	flint	6.65	0.436	55.7	0.997	179	24.1	0.309	23.5	1.65	31.4	0.621	209	82.3	0.085
	dent	6.22	0.432	57.1	0.900	168	25.1	0.302	24.3	1.91	32.0	0.557	198	82.9	0.089
Variance components															
G		0.426	0.0774	0.815	0.814	0.785	0.291	0.249	0.289	0.205	0.691	0.828	0.760	0.659	0.101
G×T		0.199	0.117	0.112	0.067	0.099	0.017	0.016	0.015	7.05E-08	0.079	0.171	0.100	0.124	0.112
G×T×R		0.199	0.279	0.105	0.026	0.121	0.231	0.018	0.216	9.29E-08	0.218	0.073	0.170	0.173	0.192
h^2		0.77	0.43	0.9	0.92	0.9	0.81	0.84	0.82	0.83	0.89	0.89	0.9	0.87	0.52
ANOVA															
T		***	***	NS	***	***	***	***	***	*	***	***	***	***	***
HetGr		NS	NS	NS	***	NS	NS	NS	NS	***	NS	NS	NS	NS	NS
T×HetGr		**	NS	.	NS	.	NS	NS	NS	NS	*	NS	NS	NS	**

., *, **, ***, NS indicate significance level of P <0.1, <0.05, <0.01, <0.001 and not significant, respectively.

Table 2 - Explanation of acronyms. Acronyms are a combination of the measured trait name (e.g. D for diameter) followed by the organ or root type as subscript (e.g. A_x for axile root).

Trait		Root order	
Name	Acronym	Name	Acronym
Diameter	D	Axile root	Ax
Dry weight	DW	Lateral root	Lat
Elongation rate	ER	Root	Rt
Relative elongation rate	k	Shoot	St
Length	L		
Number	No		
Surface area	SA		

(a_x, b_x, c_{heat},c_{cold}) and those without interactions (a_{heat}, a_{cold}, b_{opt}, b_{ex}). Class (a) displays the response of an allele to either chilling or heat stress while (b) illustrates a similar response to the temperature extremes. Furthermore, the subscript "x" denotes a crossover-interaction. Classes without interactions illustrate a response to heat- (a_{heat}), chilling- (a_{cold}), optimal- (b_{opt}) and extreme conditions (b_{ex}). Subclasses of c show a crossover-interaction combined with either a similar response to optimal and heat (c_{heat}) or to optimal and chilling (c_{cold}) conditions.

Results

Chilling had the strongest effect on growth

Chilling reduced the elongation of axile and lateral roots by 81 and 72%, respectively. Both traits were affected less by heat stress. At the end of the experiment total root length, root diameter, and root surface area had increased in plants grown under extreme temperatures. The root dry weight and the root-to-shoot dry weight ratio decreased from chilling temperature to optimum temperature to high temperature. Thus, shoot growth increased more than root growth when temperature increased. The heritability was high for all the traits (average of 0.81), with the exception of k_{Lat} (0.43) due to low genotypic variance (Table 1). When heritability was calculated separately for each heterotic group that of the flints increased slightly (average of 0.85), while that of the dents decreased (average of 0.73). The decrease in heritability in the dents was most apparent for k_{Lat}, No_{Se} and k_{Lat}/ER_{Ax} and was caused by lower genotype variance in the dents (data not shown).

Interactions among temperature and heterotic group were due to stronger elongation of axile roots of the dents at optimal temperature

Only differences in the diameter of axile roots and the number of seminal roots for the flint and the dent groups were significant (ANOVA, Table 1). On average, the axile roots of the flints were 0.09 mm (9%) thicker and the number of seminal roots was 15% lower compared to the dents. The number of seminal roots of the dents showed a lower genotypic variance, indicating less diversity among the dent lines for this trait (data not shown). Heterotic group-by-temperature treatment interactions were found for ER_{Ax}, for the ratio of the elongation rates of axile and lateral roots (k_{Lat}/ER_{Ax}), and for the total root dry weight. Compared to the flints, the dents had a 19% higher ER_{Ax} at optimum temperature, which led to axile roots being longer by 17% at the end of the experiment. In contrast, the relative growth rate of the lateral roots of the flints was higher at optimum temperature, indicated by a wider k_{Lat}/ER_{Ax} ratio. Furthermore, the flints produced more root dry matter under chilling conditions (+7% weight) and less dry matter under close-to-optimal temperatures (-7% weight).

The association analysis yielded 70 marker-trait associations with main effects for 12 traits (Supplementary Table 1). Using only associations mapped to a chromosome and combining those associations within a window of ±20 cM on the IBM2 map, 43 QTL could be reported (Figure 2). The number QTLs with main effects ranged from one for the surface area of lateral roots (SA_{Lat}) and total root length to 13 for the median diameter of the axile roots (D_{Ax}) (Figure 2). The genetic variance explained by all the markers ranged from about 27% for SA_{Lat} to 93% for the number of seminal roots (No_{Se}). The contribution of single markers was highest and lowest for No_{Se} (77.7 and 7.7%, respectively) and averaged 30.6% for all the markers of all traits. A total of 27 of the 70 associations were observed for AFLPs, which have not yet been mapped to one of the 10 chromosomes on the Keygene integrated map (NA, Supplementary Table 1).

Dents carried trait-increasing alleles for length and surface area of axile roots

The heterotic groups were compared for the frequency of alleles in the detected associations to determine whether some alleles were significantly more frequent in one heterotic group than in the other (further called group-specific alleles). Group specificity was the case for 50% of the associations with main effects, where the frequency of alleles differed among the groups (Supplementary Table 1, χ^2). In the flints, an allele was fixed in six cases; five of the fixed alleles were for the number of seminal roots (Supplementary Table 1). An allele was absent in six cases without trait specificity. The frequency of most of the trait-decreasing alleles at loci controlling axile root length (L_{Ax}), surface area of the axile roots (SA_{Ax}), and total root surface area (SA_{Rt}) was significantly higher in the flints.

Alleles effects predominantly showed similar response to temperature-extremes

The allele substitution effect ($\alpha 1/2$) among each trait and treatment was of a similar magnitude for most detected associations, with the exception of ER_{Ax} (16°C). However, $\alpha 1/2$ differed strongly between the temperature treatments for each trait and within the treatments. We classified the detected marker-by-temperature interactions according to the allele response classes based on $\alpha 1/2$ (Figure 3). The majority of alleles responded with at least one crossover interaction (Table 3, a_x, b_x, c_{heat}, or c_{cold}). The type of

allele response to temperature can be examined best for the two traits with the highest number of detected associations, i.e. ER_{Ax} (50 associations) and k_{Lat}/ER_{Ax} (28 associations) (Table 3). For ER_{Ax}, most of the responses were assigned to scenario 'b' indicating similar allele responses to temperature extremes. Among these, 30% showed an interaction (b_x) and 24% showed sizable effects at optimal temperature (b_{opt}). There were nine loci, where the change in the relative effect on trait values was above 6% at optimal temperatures. These were detected in bins 5.01, 5.03, 7.02, and 10.04, to mention only those mapped to a chromosome. Under chilling, there were four sizable loci, with only one being mapped to a chromosome (bin 7.02). Under high temperature, no sizable locus was detected. For k_{Lat}/ER_{Ax}, all the responses were assigned to b_x (82%) and c_{cold} (18%) (Table 3). The effect of most loci was around 20% at the control temperature. A closer look at the c_{cold}-type responses revealed that they were similar to b_{opt}- or b_x-type responses with a large effect at the control temperature and small or even negative effects at extreme temperatures. Thus, the majority of loci showed a clear effect at the control temperature but weak or invers effects at the extremes. One remarkable locus (bin 10.04) caused a particularly strong change in root morphology at extreme temperatures (b_x). A negative collocation was observed for two markers (bin 10.04) for ER_{Ax} and k_{Lat}/ER_{Ax}. Furthermore, the effect flint (Supplementary Table 2) indicated greater tolerance of ER_{Ax} to temperature extremes but lesser tolerance of k_{Lat} and, accordingly, a decrease in k_{Lat}/ER_{Ax}.

Flints carried alleles favoring chilling tolerance of root dry weight; dents carried alleles for higher k_{Lat}/ER_{Ax} at heat

There were 90 marker-by-temperature interactions for 12 traits (Supplementary Table 2). Using only associations mapped to a chromosome and combining those associations within a window of 20 cM on the IBM2 map, 40 QTL could be reported (Figure 2). The number of QTLs ranged from one for the median diameter of both root types (D_{Ax}, D_{Lat}) to 20 for ER_{Ax} (Figure 2). Thirty-two of the 90 associations were observed for AFLPs, which have not yet been mapped to one of the 10 chromosomes on the Keygene integrated map (NA, Supplementary Table 2). Group specificity was the case for 83.3% of the marker-by-temperature interactions (Supplementary Table 2, χ^2). At most of the group-specific loci, there was a clear association of the tolerance-increasing allele to one of the heterotic groups. For most marker-trait associations, the flint group carried the allele increasing tolerance to heat and cold; for k_{Lat}/ER_{Ax}, the flint group carried the allele decreasing tolerance to heat and cold. Thus, all these associations were clearly trait and group specific. The croup-specificity of these associations is supported by a similar behavior of the mean values of each heterotic group in response to temperature (cf Table 3).

Response of ER_{Ax} to temperature altered root morphology as indicated by k_{Lat}/ER_{Ax}

The detected associations were projected onto the IBM2 2008 Neighbors Frame genetic map. Collocations of marker-trait associations were detected on all chromosomes (Figure 2). Collocations for association-by-temperature interaction effects were found to a greater extent for axile root traits. Eleven collocations between ER_{Ax} and k_{Lat}/ER_{Ax} appeared on different chromosomes (Figure 2). A positive collocation between the ratio k_{Lat}/ER_{Ax} and k_{Lat} was detected in only one case (bin 10.04) (Supplementary Table 2), indicating that a change in ER_{Ax} generally influenced this ratio. This is supported by the close negative correlation between ER_{Ax} and k_{Lat}/ER_{Ax} ($r \sim -0.74$), while k_{Lat} was not correlated with the ratio and, thus, did not influence the ratio. Two collocations for k_{Lat}/ER_{Ax} and axile root length (L_{Ax}) were detected in bins 2.09 (negative collocation) and 10.04 (positive collocation) (Supplementary Table 2, Figure 2). Collocations for associations with main effects were found for several traits. On chromosome 5, the surface area of axile roots (SA_{Ax}) and the total root surface area (SA_{Rt}) collocated positively with the ratio between the dry weight of the root and the shoot in bin 5.05. In bin 6.08, SA_{Ax} and SA_{Rt} collocated positively with total root dry weight. This is supported by the high correlations between these traits ($r \sim 0.7$). In bin 7.02, the surface area of the lateral roots (SA_{Lat}), the length of axile roots (L_{Ax}), and the total root surface area (SA_{Rt}) were collocated. Accordingly, the correlation of L_{Ax} and SA_{Rt} was close ($r \sim 0.9$), but lateral roots also played a major role in determining root surface area ($r \sim 0.7$).

Linked genes involved in temperature response mechanisms

Genes close to the detected association (± 20 cM region), which are involved in temperature-tolerance mechanisms, were selected from the IBM2 2008 Neighbors Frame map (MaizeGDB: http://www.maizegdb.org/). In bin 1.05, glutathione S-transferase *Gst32* and *Gst42* were located ~12 cM and *Gst14* was ~5 cM from an association for ER_{Ax}. In bin 8.05, *Gst15* was 2 cM from a marker-by-temperature interaction for ER_{Ax}. In bin 1.04, sucrose synthase (*Sus2*) (pos 329.06 cM) was in 13 cM from marker-by-temperature interactions for ER_{Ax} and k_{Lat}/ER_{Ax} (Figure 2). In bin 9.04 *Sus1* was 8 cM from a cluster of ER_{Ax} and k_{Lat}/ER_{Ax} associations. *Vacuolar acid invertase2* (*Ivr2*) (bin 5.03, 288 cM) was 3 cM from a marker-by-temperature interaction for ER_{Ax} (type b_{opt} response). The second gene in bin 5.04, *cell wall invertase1* (*Incw1*) (376.4 cM), was 1 cM from a marker-by-temperature interaction for ER_{Ax}. *Incw3* (bin 10.04, 272.2 cM), from the same gene family, was 7 cM from a cluster of marker-by-temperature interactions for ER_{Ax}, k_{Lat}, L_{Ax}, and k_{Lat}/ER_{Ax}. *Sus*, *Ivr*, and *Incw* all provide sucrose cleavage mechanisms so that sugars can be transported to and utilized in the sink organs.

In bin 1.08, a gene coding for a glycine-rich protein (*Grp1*) was only 2 cM from an association for D_{Lat} and 4 cM from a marker-by-temperature interaction for ER_{Ax}. In bin 5.03, a similar gene, *Grp3* (243.5 cM), was 1 cM from a marker-by-temperature interaction for ER_{Ax} and 2 cM from an association for No_{Se}.

Discussion

Root growth and Morphology

Fewer seminal roots and a larger median diameter of axile roots was associated with the flints, as observed too by Wiggans (1916). Wiggans also found that flints had only one to two seminal roots, whereas the dents had three to four seminal roots. This difference was also described by Hoecker et al (2006). Seedlings grown at 15°C had thicker roots with considerably fewer hairs than roots grown at higher temperature (Cutforth et al, 1986). Therefore, the increased diameter of the flints may be a strategy to achieve tolerance to chilling, because thicker roots enable better water transport under chilling stress due to xylem vessels with a greater diameter (Varney et al, 1991).

Root elongation vs. final root length

We found a greater number of marker-by-temperature interactions for traits related to root elongation rates than was found for measurements at the end of the experiment. For example, ER_{Ax} yielded 50 associations compared to L_{Ax}, which had only two. The detection of fewer associations for L_{Ax} may be due to unaccounted differences in germination. These differences can result in large errors and can be overcome

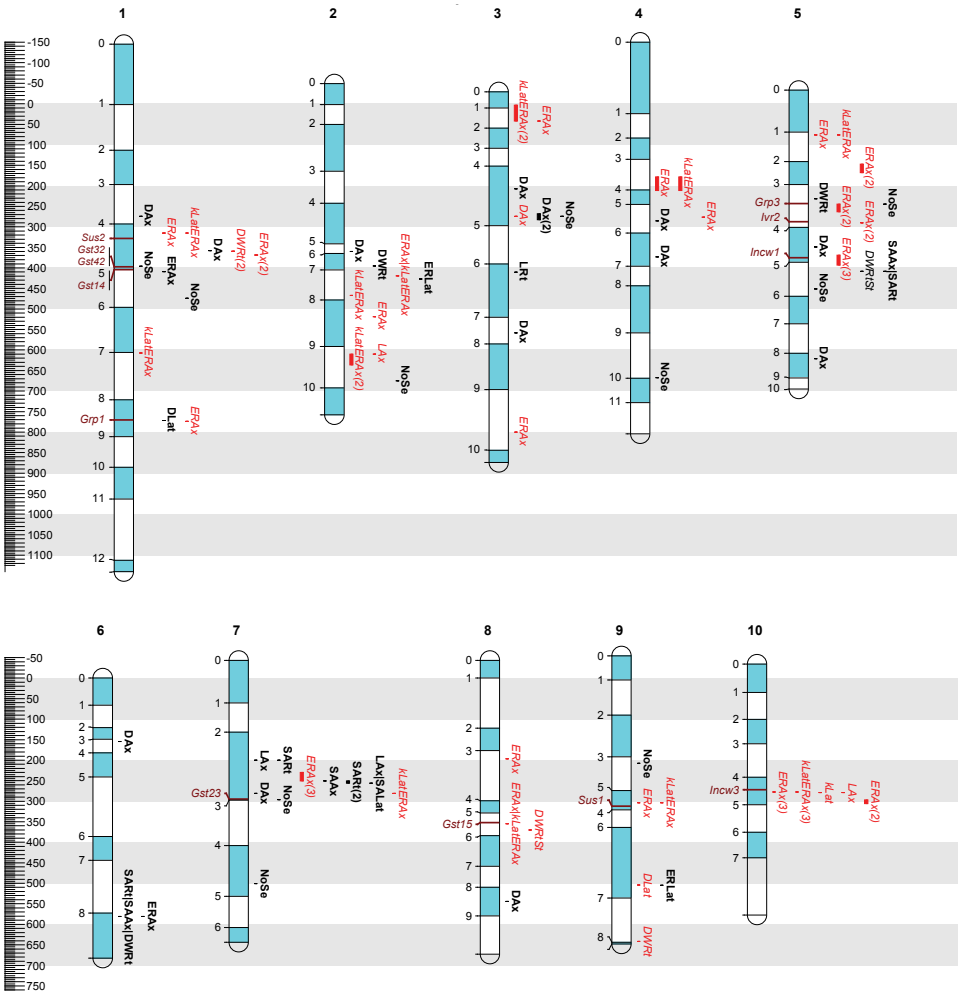

Figure 2 - Detected QTLs projected on the on the IBM2 2008 Neighbors Frame reference map (MaizeGDB: http://www.maizegdb.org/). The scale indicates the position on the reference map in cM. Labels to the left of each chromosome indicate the bin numbers (shaded areas) as well as candidate genes mentioned in the text. Candidate genes are *glutathione S-transferase* (*Gst*), *sucrose synthase* (*Sus*), *Vacuolar acid invertase* (*Ivr*) and *cell wall invertase* (*Incw*). Marker-by-trait associations are listed at the right of the chromosomes. In case several association of the same trait fell within a window of ±20 cM, these associations were combined and the interval between the first and the last association was given. The number of combined associations is given in brackets. Marker-trait associations with main effects are indicated in bold type; marker-by-temperature interactions are italicized. For trait abbreviation see Table 2.

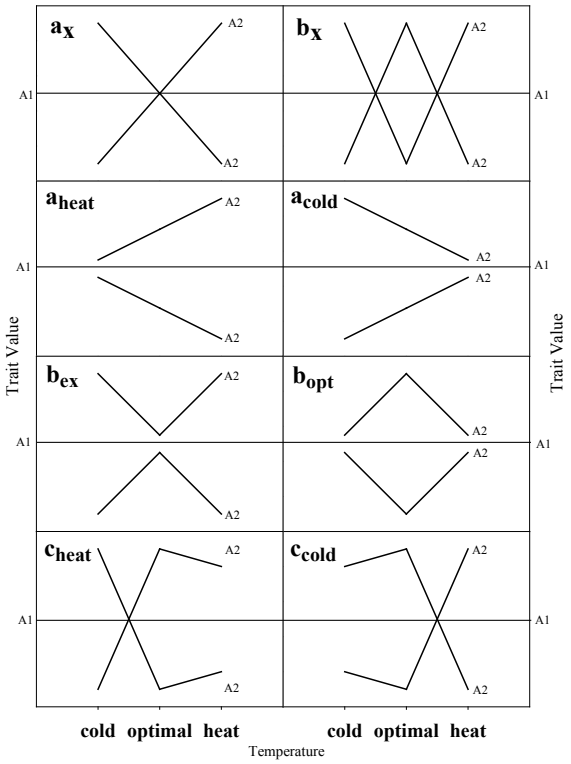

Figure 3 - Classification of AFLP allele response based on the relative allele substitution effects ($\alpha 1/2$) in each temperature treatment. A2 shows two possible reactions of one allele in relation to the reference allele (A1 zero line). Alleles confer tolerance to temperature extreme (a), or to both temperature extremes (b), and indifferent (c). Classes are subdivided into crossover interactions (a_x, b_x) and no crossover interactions but responsive to heat (a_{heat}), chilling (a_{cold}), optimal (b_{opt}) and extreme conditions (b_{ex}). Subclasses of c show either a similar response to optimal heat (c_{heat}) or to optimal chilling (c_{cold}) conditions.

by measuring elongation rates (Hund et al, 2009). The detection of a greater number of marker-by-environment interactions resulting from the measurement of elongation rates is corroborated by a QTL study of the response of root elongation to water deficit (Ruta et al, 2010).

The response was alleles is similar at both temperature extremes

The relative allele effects were usually strongest at the optimum temperature, decreased towards the extremes (b_{opt}), and sometimes reverted into the opposite effect (b_x). The pattern of allele response of bx and the subclasses (Figure 3) indicates that genotypes are 'equipped' with alleles that are superior or inferior at both temperature extremes in contrast to the optimum. Thus, relative differences in growth rates at extreme temperatures might be due to the activation of stress-response pathways. These may help to maintain organ growth or, alternatively, stop organ growth as we observed. The effect of the largest genetic differences at optimal temperature is confirmed again by the differences between the heterotic groups. The contribution of the alleles to temperature tolerance is best explained by k_{Lat}/ER_{Ax} and ER_{Ax}, which showed most marker-by-temperature interactions. In the case of k_{Lat}/ER_{Ax}, the inversion of the relative allele effect from the extremes to the close-to-optimal temperature was strong and affected many loci. Furthermore, an increase in k_{Lat}/ER_{Ax} was frequently collocated with a decrease in ER_{Ax}. The relative increase at these loci might be due to the effect of temperature on the growing meristem of the axile root, not on the lateral root. Hund et al (2008) also found that the overall length of the lateral roots was not influenced by temperature. This may be related to apical dominance and to compensation for stress effects on the axile root meristem by subsequent lateral roots. An increase in lateral roots was also observed when roots grew at very high concentrations of PEG, which caused a very low water potential (Trachsel et al, 2010b). Longer lateral roots have been associated with better plant performance at low temperature (Hund et al, 2007) and are considered to be a key factor in improving early vigor (Hund et al, 2008).

In the case of ER_{Ax}, the majority of alleles showed the strongest effects under chilling stress and weaker effects at optimum temperature. This might suggest that alleles responsible for cold tolerance can have a negative effect on plant growth at optimal temperature. This phenomenon has been described for photosynthesis-related traits (Jompuk et al, 2005), but not yet for root elongation.

Allelic composition of heterotic groups

We decided to report also markers for which the alleles were not detected as polymorphic in the standard mapping populations of Keygene. Since we do not know if these markers map to the same or different haplotype blocks, the numbers give only an upper estimate of the true number of associations. However, for almost all traits, the alleles were clearly group-specific, i.e. all trait-increasing alleles tended to be more abundant in one of the heterotic groups. This is remarkable, because these associations were detected, despite the fact that the population structure was taken into account. Thus, only those associations were detected, for which the marker was not fully associated with the heterotic group. If population structure is not considered, then the detection of false positive associations cannot be avoided (Andersen et al, 2005; Camus-Kulandaivelu et al, 2006). On the other hand, fixed alleles for the target trait are closely associated with population structure (heterotic group) and might not be detected if population structure were considered (Andersen et al, 2005; Camus-Kulandaivelu et al, 2006). When population structure was not taken into account, there was an increase in the number of detected main marker-trait associations with main effects (142 compared to 70), probably due mainly to a high number of false posi-

Table 3 - List of allele response classes for marker-by-temperature interactions. See Table 2 for abbreviations of traits. Symbols refer to the list of classes in Figure 3.

		Percentages of allele response classes							
Trait	No. marker with sig. temperature interaction effects	c_{cold}	a_x	b_x	a_{heat}	a_{cold}	b_{ex}	b_{opt}	c_{heat}
k_{Lat}	2	-	100	-	-	-	-	-	-
ER_{Ax}	50	-	30	-	16	-	24	12	18
L_{Ax}	2	-	100	-	-	-	-	-	-
D_{Ax}	1	-	-	-	-	-	-	-	100
D_{Lat}	1	100	-	-	-	-	-	-	-
DW_{Rt}	4	-	50	-	-	25	-	25	-
DW_{RtSt}	2	-	50	-	-	-	-	-	50
k_{Lat}/ER_{Ax}	28	-	82	-	-	-	-	-	18

tives. In the case of marker-trait associations, which interacted with temperature, taking the population structure into account did not increase the number of detections (90 vs 89). Thus, it is unlikely that true response alleles were discarded when accounting for population structure.

The detected group specificity is remarkable since it is unlikely that it would happen by chance. But what causes a "synchronized" unequal distribution of the trait-increasing alleles in both heterotic groups? Our results indicate that the heterotic groups may have been selected to allow for a wider adaptation to temperature by the resulting hybrid. The flint contributed alleles for chilling tolerance, and the dent lines contributed to productivity under optimal conditions and, thus, to a high yield potential (Hallauer, 1990). However, little is known about how modern flint and dent lines differ with respect to their allelic contribution to temperature tolerance. Mc William and Griffing (1965) evaluated the temperature-dependence of heterosis in maize and its contribution to hybrid vigor. They compared a northern flint inbred line with a southern dent inbred line and did not find strong differences among them. One reason for this might have been the reported genetic defect in the flint line due to inbreeding, which affected the formation of chlorophyll, especially in the cold. Hund et al (2012) provided the prove-of-concept that hybrids of flint and dent inbred lines with different temperature-behavior perform better across the sum of all temperatures the hybrid is exposed to. However, they evaluated only a small set of reciprocal crosses between two flint and two dent inbred lines. Based on the study of Hund et al (2012), it cannot be generalized that the combination of genotypes with different temperature behavior will lead to improved hybrids. However, the results obtained here suggest that different temperature behavior is the case in the flint-dent heterotic breeding pool: While the dents are characterized by an increased root growth at optimal temperature, the flints show slightly increased root growth at temperature-extremes. It will be interesting to evaluate, if the most contrasting inbred lines will lead to superior hybrids better adapted to various temperature regimes.

Candidate pathways and their genes

A high proportion of genes located around the detected associations are related to glycolysis, suggesting that this pathway plays a key role in response to temperature. It is striking that three out of six invertase genes (soluble *Ivr1* and *Ivr2*, insoluble *Incw1*, *2*, *3*, and *4*) and two of out of three sucrose synthase genes (*sus1*, *sus2*, and *sh1*) known in maize mapped close to root loci controlling the response of roots growth to temperature. Invertase and sucrose synthase are the starting enzymes of the cytosolic glycolysis pathway, which enables essential metabolic adaptability facilitating plant development (Fernandes et al, 2008; Ruan, 2012) and acclimation to environmental stress (Fernandes et al, 2008). This network seems to play a pivotal role in regulating the response to multiple types of abiotic stress. The expression of stress-specific isozymes may be regulate this pathway (Fernandes et al, 2008) with glucose being the potential signaling molecule (Roitsch and Gonzalez, 2004). The accumulation of sugars like sucrose is one of the most commonly observed responses to abiotic stress (Lunn and Furbank, 1999) and is also observed under chilling (Verheul et al, 1995). The root tips accumulate assimilated carbon to a greater extent than at optimal temperature, indicating that they cannot utilize the carbohydrates for growth and respiration (Nagel et al, 2009). An important regulatory role of invertase and sucrose synthase has already been shown for the root elongation of Arabidopsis (Sergeeva et al, 2006). One of our candidate genes, *Ivr2*, was identified as a candidate gene in a study on the genetic control of acclimation of the photosynthetic apparatus to low temperature at night (Guerra-Peraza et al, 2010).

Genes encoding for glycine-rich proteins were closely linked with root traits like D_{Lat} and ER_{Ax}. Glycine-rich proteins are root-tissue specific and

thought to be proteins of the cell wall (Goddemeier et al, 1998). Grp synthesis is induced by external stimuli like abscisic acid (ABA) (De Oliveira et al, 1990; Godoy et al, 1990). Since ER_{Ax} is a response association and is usually classified as b_x and b_{opt} and since chilling stress is accompanied by an increase in the ABA concentration, Grp might be an appropriate candidate for selecting genotypes with the expression of large amounts of Grp in the roots.

Conclusions

Most of the differences between the heterotic groups were at optimal temperature: the dents grew longer axile roots, and the flints produced a relatively larger proportion of lateral roots. This pattern was also observed for the detected marker-trait associations. The dents carried more alleles increasing ER_{Ax} and more alleles increasing the sensitivity of ER_{Ax} to temperature extremes. In general, the majority of alleles showed a similar response to cold and heat (b_{opt} and b_x). The inverted allele effect (b_x) at many loci indicates that the favorable effect of the different alleles depends on temperature. The development of the heterotic groups was based on the selection of hybrids, i.e. only parents with good combining ability were retained in the groups. This raises the question as to whether the combination of alleles with different responses to temperature would enable the adaptation of the hybrid to a wider range of temperature. A good locus to test this hypothesis is that in bin 10.04, which has a temperature dependent effect on overall root morphology.

References

Andersen JR, Schrag T, Melchinger AE, Zein I, Lubberstedt T, 2005. Validation of Dwarf8 polymorphisms associated with flowering time in elite European inbred lines of maize (*Zea mays* L). Theor Appl Genet 111: 206-217

Arcade A, Labourdette A, Falque M, Mangin B, Chardon F, Charcosset A, Joets J, 2004. BioMercator: integrating genetic maps and QTL towards discovery of candidate genes. Bioinformatics 20: 2324-2326

Barreto HJ, Edmeades GO, Chapman SC, Crossa J, 1997. The alpha lattice design in plant breeding and agronomy: Generation and analysis, pp. 544-551 In: Developing drought and low N-tolerant maize. Edmeades GO, Bänziger M, Mickelson HR, Peña-Valdivia CB, eds. Proceedings of a symposium, El Batan, Mexico

Camus-Kulandaivelu L, Veyrieras JB, Madur D, Combes V, Fourmann M, Barraud S, Dubreuil P, Gouesnard B, Manicacci D, Charcosset A, 2006. Maize adaptation to temperate climate: Relationship between population structure and polymorphism in the Dwarf8 gene. Genetics 172: 2449-2463

Cutforth, HW, Shaykewich CF, Cho CM, 1986. Effect of Soil-Water and Temperature on Corn (Zea Mays L) Root-Growth During Emergence. Can J Soil Sci 66: 51-58

De Oliveira DE, Seurinck J, Inze D, Van Montagu M, Botterman J, 1990. Differential Expression of Five Arabidopsis Genes Encoding Glycine-Rich Proteins. Plant Cell 2: 427-436

Engels C, 1994. Effect of root and shoot meristem temperature on shoot to root dry matter partitioning and the internal concentrations of nitrogen and carbohydrates in maize and wheat. Ann Bot 73: 211-219

Fernandes J, Morrow DJ, Casati P, Walbot V, 2008. Distinctive transcriptome responses to adverse environmental conditions in Zea mays L. Plant Biotechnol J 6: 782-798.

Flint-Garcia SA, Thornsberry JM, Buckler ES, 2003. Structure of linkage disequilibrium in plants. An nu Rev Plant Biol 54: 357-374.

Fracheboud Y, Haldimann P, Leipner J, Stamp P, 1999. Chlorophyll fluorescence as a selection tool for cold tolerance of photosynthesis in maize (Zea mays L). J Exp Bot 50: 1533-1540

Frei OM, 2000. Changes in yield physiology of corn as a result of breeding in northern Europe. Maydica 45: 173-183

Gilmour A, Gogel B, Cullis B, Thompson R, 2006. ASReml user guide release 2.0. VSN International Ltd, Hermel Hempstead.

Goddemeier ML, Wulff D, Feix G, 1998. Root-specific expression of a *Zea mays* gene encoding a novel glycine-rich protein, zmGRP3. Plant Mol Biol 36: 799-802

Godoy JA, Pardo JM, Pintortoro JA, 1990. A Tomato Cdna Inducible by Salt Stress and Abscisic-Acid - Nucleotide-Sequence and Expression Pattern. Plant Mol Biol 15: 695-705

Gower JC, 1966. Some distance properties of latent root and vector methods used in multivariate analysis. pp. 325-326

Guerra-Peraza, O, Leipner J, Reimer R, Nguyen HT, Stamp P, FrachboudY, 2010. Temperature at night affects the genetic control of acclimation to cold in maize seedlings. Maydica 56: 367-377

Hallauer AR, 1990. Methods used in developing maize inbreds. Maydica 35: 1-16

Hoecker N, Keller B, Piepho HP, Hochholdinger, F, 2006. Manifestation of heterosis during early maize (*Zea mays* L) root development. Theor Appl Genet 112: 421-429

Holland J, Nyquist W, Cervantes-Martínez C, 2003. Estimating and Interpreting Heritability for Plant Breeding: An Update, pp. 9-112. In: Plant Breeding Reviews, vol 22. John Wiley & Sons Inc

Holm S, 1979. A Simple Sequentially Rejective Multiple Test Procedure. Scand J Stat 6: 65-70

Hund A, Frachboud Y, Soldati A, Frascaroli E, Salvi S, Stamp P, 2004. QTL controlling root and shoot traits of maize seedlings under cold stress. Theor

Appl Genet 109: 618-629
Hund A, Fracheboud Y, Soldati A, Stamp P, 2008. Cold tolerance of maize seedlings as determined by root morphology and photosynthetic traits. Eur J Agron 28: 178-185
Hund A, Reimer R, Messmer R, 2011. A consensus map of QTLs controlling the root length of maize. Plant Soil 344: 143-158
Hund A, Reimer R, Stamp P, Walter A, 2012. Can we improve heterosis for root growth of maize by selecting parental inbred lines with different temperature behaviour? Phil Trans R Soc B 367: 1580-1588
Hund A, Richner W, Soldati A, Fracheboud Y, Stamp P, 2007. Root morphology and photosynthetic performance of maize inbred lines at low temperature. Eur J Agron 27: 52-61
Hund A, Trachsel S, Stamp P, 2009. Growth of axile and lateral roots of maize: I development of a phenotyping platform. Plant Soil 325: 335-349
Jompuk C, Fracheboud Y, Stamp P, Leipner J, 2005. Mapping of quantitative trait loci associated with chilling tolerance in maize (*Zea mays* L) seedlings grown under field conditions. J Ex Bot 56: 1153-1163
Lawrence CJ, Seigfried TE, Brendel V, 2005. The Maize Genetics and Genomics Database. The Community Resource for Access to Diverse Maize Data. Plant Physiol 138: 55-58
Lunn JE, FurbankRT, 1999. Sucrose biosynthesis in C-4 plants. New Phytol 143: 221-237
McCully ME, 1999. Roots in soil: unearthing the complexities of roots and their rhizospheres. Annu Rev Plant Physiol Plant Mol Biol 50: 695-718
McWilliam JR, Griffing B, 1965. Temperature-Dependent Heterosis in Maize. Aus J Biol Sci 18: 569-583
Nagel KA, Kastenholz B, Jahnke S, Van Dusschoten D, Aach T, Muhlich M, Truhn D, Scharr H, Terjung S, Walter A, Schurr U, 2009. Temperature responses of roots: impact on growth, root system architecture and implications for phenotyping. Func Plant Biol 36: 947-959
Nietosotelo J, Ho THD, 1986. Effect of Heat-Shock on the Metabolism of Glutathione in Maize Roots. Plant Physiol 82: 1031-1035.
Piepho HP, 2000. A mixed-model approach to mapping quantitative trait loci in barley on the basis of multiple environment data. Genetics 156: 2043-2050
Pritchard JK, Stephens M, Rosenberg NA, Donnelly P, 2000. Association mapping in structured populations. Am J Hum Genet 67: 170-181
R Development Core Team, 2008 R: A language and environment for statistical computing. R Foundation for Statistical Computing, Vienna, Austria
Rogers JS, 1972. Measures of Genetic Similarity and Genetic Distance, pp. 145-153. In: Studies in Genetics, vol 7. Marshall R ed. University of Texas, Austin, TX
Roitsch T, Gonzalez MC, 2004. Function and regulation of plant invertases: sweet sensations. Trends Plant Sci 9: 606-613
Ruan YL, 2012. Signaling Role of Sucrose Metabolism in Development. Mol Plant 5: 763-765
Ruta N, Liedgens M, Fracheboud Y, Stamp P, Hund A, 2010. QTLs for the elongation of axile and lateral roots of maize in response to low water potential. Theor Appl Genet 120: 621-631
Schaeffer ML, Sanchez-Villeda H, Coe E, 2008. Neighbors 2008 - Maize Genetics and Genomics Database
Schrag TA, Möhring J, Melchinger AE, Kusterer B, Dhillon BS, Piepho HP, Frisch M, 2010. Prediction of hybrid performance in maize using molecular markers and joint analyses of hybrids and parental inbreds. Theor Appl Genet 120: 451-461
Sergeeva LI, Keurentjes JJB, Bentsink L, Vonk J, van der Plas LHW, Koornneef M, Vreugdenhil D, 2006. Vacuolar invertase regulates elongation of Arabidopsis thaliana roots as revealed by QTL and mutant analysis. Proc Natl Acad Sci USA 103: 2994-2999
Shaw RH, 1988. Climate Requirement, pp. 609-638. In: Corn and Corn Improvement, 3rd edition. Dudley JW ed. American Society of Agronomy, Madison, Wisconsin, USA
Stich B, Melchinger AE, Heckenberger M, Möhring J, Schechert A, Piepho HP, 2008a. Association mapping in multiple segregating populations of sugar beet (*Beta vulgaris* L). Theor Appl Genet 117: 1167-1179
Stich B, Möhring J, Piepho HP, Heckenberger M, Buckler ES, Melchinger AE, 2008b. Comparison of mixed-model approaches for association mapping. Genetics 178: 1745-1754
Stone PJ, Sorensen IB, Jamieson PD, 1999. Effect of soil temperature on phenology, canopy development, biomass and yield of maize in a cool-temperature climate. Field Crop Res 63: 169-178.
Timperio AM, Egidi MG, Zolla L, 2008. Proteomics applied on plant abiotic stresses: Role of heat shock proteins (HSP). J Proteomics 71: 391-411
Trachsel S, Messmer R, Stamp P, Hund A, 2009. Mapping of QTLs for lateral and axile root growth of tropical maize. Theor Appl Genet 119: 1413-1424
Trachsel S, Stamp P, Hund A, 2010a. Effect of high temperatures, drought and aluminum toxicity on root growth of tropical maize (*Zea mays* L) Seedlings. Maydica 55: 249-260
Trachsel S, Stamp P, Hund A, 2010b. Growth of axile and lateral roots of maize: response to desiccation stress induced by polyethylene glycol 8000. Maydica 55: 101-109
Tuberosa R, Salvi S, Sanguineti MC, Maccaferri M, Giuliani S, Maccaferri M, Sanguineti MC, Landi P, 2003. Searching for quantitative trait loci control-

ling root traits in maize: a critical appraisal. Plant Soil 255: 35-54

Varney GT, Canny MJ, Wang XL, McCully ME, 1991. The branch roots of Zea. 1. 1st order branches, their number, sizes and division into classes. Ann Bot 67: 357-364

Verheul MJ, Vanhassel PR, Stamp P, 1995. Comparison of Maize Inbred Lines Differing in Low-Temperature Tolerance - Effect of Acclimation at Suboptimal Temperature on Chloroplast Functioning. Ann Bot 76: 7-14

Wallace B, 2000. A Natural Historian's View of Heterosis and Related Topics, pp. 41-45. In: Evolutionary Genetics: from molecules to morphology. Singh RP, Krimbas CB eds. Cambridge University Press, Camebridge

Wiggans RG, 1916. The number of temporary roots in cereals. J Am Soc Agron 8: 31-37

Zhao K, Aranzana MJ, Kim S, Lister C, Shindo C, Tang CL, Toomajian C, Zheng HG, Dean C, Marjoram P, Nordborg M, 2007. An Arabidopsis example of association mapping in structured samples. Plos Genetics 3

Supplementary Table 1

Associations with main effects							χ^2 two sample test Flint/Dent	Ratio Flint		Effect Flint on trait increase
Trait	Marker	Pos. KG (cM)	Pos. IBM (cM)	Bin	p_g (%)	α½		Allele 1	Allele 2	
ER_{Ax}	269	77.4	410	1.05	30.9	-7.65	NS	0.43	0.44	-
	318	126	581	6.08	28.7	-10.1	***	0.31	0.83	-
	927	NA	NA	NA	28.2	-10.1	***	0	0.57	-
	1263	NA	NA	NA	28.4	6.51	NS	0.25	0.49	+
	710	NA	NA	NA	33.9	17.3	***	0.96	0.11	-
				total	79.5					
L_{Ax}	962	51.3	200	7.02	27.9	4.38	***	0.96	0.11	-
	294	56.4	256	7.02	28.3	4.18	***	0.93	0.09	-
	710	NA	NA	NA	31.3	4.89	***	0.96	0.11	-
				total	30.3					
D_{Ax}	1548	57	275	1.03	29.4	4.16	NS	0.41	0.45	+
	972	69.7	359	1.04	25.5	-4.60	NS	0.7	0.4	+
	2169	84.1	361	2.05	30.3	4.43	NS	0.42	0.44	+
	869	51.6	208	3.04	29.7	4.27	NS	0.39	0.47	+
	2036	57.8	269	3.04	29.4	4.16	NS	0.41	0.45	+
	587	59.2	283	3.04	29.4	4.16	NS	0.41	0.45	+
	2133	104	559	3.07	25.6	-3.93	NS	0.44	0.42	+
	753	61.4	286	4.05	30.4	3.85	NS	0.42	0.43	+
	1101	79.4	374	4.06	24.5	3.86	*	0.65	0.33	-
	1113	81.2	350	5.04	31.3	3.81	NS	0.34	0.45	+
	2158	141	622	5.08	29.4	4.16	NS	0.41	0.45	+
	661	44.1	155	6.02	29.4	-4.16	NS	0.45	0.41	+
	336	59.5	281	7.02	25.1	5.24	NS	0.33	0.47	+
	2047	129	544	8.08	26.2	3.74	NS	0.42	0.44	+
	1541	NA	NA	NA	29.4	4.16	NS	0.41	0.45	+
	1829	NA	NA	NA	25.6	3.86	NS	0.4	0.4	=
	2049	NA	NA	NA	25.6	3.93	NS	0.42	0.44	+
	2054	NA	NA	NA	29.7	4.27	NS	0.39	0.47	+
	2058	NA	NA	NA	29.7	4.27	NS	0.39	0.47	+
	2083	NA	NA	NA	29.4	4.16	NS	0.41	0.45	+
	2086	NA	NA	NA	23.4	3.85	NS	0.45	0.42	-
	2089	NA	NA	NA	29.6	4.23	NS	0.42	0.44	+
	2117	NA	NA	NA	29.0	4.07	NS	0.39	0.47	+
	2123	NA	NA	NA	29.4	4.16	NS	0.41	0.45	+
				total	51.5					
SA_{Ax}	767	93.9	409	5.05	28.1	-0.565	*	0	0.51	-
	318	126	581	6.08	24.8	-0.656	***	0.31	0.83	-
	544	55.8	251	7.02	22.4	0.696	***	0.93	0.13	-
	710	NA	NA	NA	28.7	0.906	***	0.96	0.11	-
				total	61.6					
D_{Lat}	542	123	773	1.08	30.7	-4.81	NS	0.45	0.38	+
	543	NA	NA	NA	30.7	4.81	NS	0.38	0.45	+
	1365	NA	NA	NA	29.8	4.71	NS	0.38	0.46	+

				total	29.8					
SA_{Lat}	294	56.4	256	7.02	27.3	1.12	***	0.93	0.09	-
No_{Se}	308	75.4	397	1.04	8.78	-13.2	NS	0.67	0.42	+
	129	83.6	475	1.05	51.1	6.80	*	1	0.36	-
	832	151	676	2.09	7.71	-6.56	**	0.92	0.34	+
	1177	58.4	275	3.04	72.5	-1.93	**	1	0.36	+
	1371	140	668	4.09	70.0	2.45	NS	0.48	0.4	-
	930	64	245	5.03	17.0	-5.44	***	0.1	0.34	+
	1253	102	452	5.05	72.2	-2.73	NS	0.13	0.46	-
	1776	63.6	296	7.02	35.1	2.15	**	0.68	0.28	-
	560	102	501	7.04	18.8	-5.89	***	0.81	0.22	+
	1059	68.5	208	9.03	15.2	-11.1	*	1	0.39	+
	1247	NA	NA	NA	31.0	7.08	**	1	0.38	-
	1379	NA	NA	NA	54.7	2.69	NS	0.39	0.83	+
	1382	NA	NA	NA	77.7	3.37	***	0.22	0.91	+
	1465	NA	NA	NA	22.5	12.4	NS	1	0.41	-
	1790	NA	NA	NA	4.61	-5.87	NS	0.51	0.24	+
				total	92.6					
DW_{Rt}	639	91	396	2.06	38.0	-1.72	*	0.07	0.51	-
	467	61.8	232	5.03	22.6	0.84	***	0.65	0.07	-
	318	126	581	6.08	26.4	-0.98	***	0.31	0.83	-
	94	NA	NA	NA	28.8	-1.89	**	0	0.54	-
				total	60.6					
SA_{Rt}	767	93.9	409	5.05	25.4	-0.475	*	0	0.51	-
	318	126	581	6.08	25.7	-0.579	***	0.31	0.83	-
	962	51.3	200	7.02	25.8	0.723	***	0.96	0.11	-
	544	55.8	251	7.02	23.3	0.628	***	0.93	0.13	-
	294	56.4	256	7.02	25.2	0.680	***	0.93	0.09	-
	755	NA	NA	NA	23.2	0.752	***	1	0.13	-
	710	NA	NA	NA	29.8	0.818	***	0.96	0.11	-
				total	58.6					
L_{Rt}	217	85.2	411	3.06	31.5	-0.129	**	0.32	0.8	-
DW_{RtSt}	767	93.9	409	5.05	35.2	-19.8	*	0	0.51	-
	1356	NA	NA	NA	31.5	22.3	***	0.65	0	-
				total	53.1					
k_{Lat}/ER_{Ax}	1379	NA	NA	NA	44.2	5.44	NS	0.39	0.83	+

*, **, ***, NS indicate significance level of P <0.05, <0.01, <0.001 and not significant, respectively, based on a χ^2 two sample test for allele distribution between the heterotic groups.

[NA]: Marker is not yet mapped to one of the 10 chromosomes on the Keygene integrated map.

Supplementary table 2

Marker-by-temperature interactions					α1/2			allele response class	χ^2 two sample test Flint/ Dent	Ratio Flint		Effect Flint	
Trait	Marker	Pos. KG (cM)	Pos. IBM (cM)	bin	16 °C	28 °C	36 °C			Allele 1	Allele 2	cold	heat
k_{Lat}	765	60.4	279	10.04	-18.9	14.1	-0.52	b_x	**	0.17	0.6	-	-
	1786	NA	NA	NA	19.6	-21.2	4.01	b_x	**	0	0.52	+	+
ER_{Ax}	31	63.2	316	1.04	-14.4	-10.9	-3.25	a_{cold}	***	0	0.57	-	+
	473	71.2	369	1.04	0.84	5.69	-4.51	c_{cold}	***	0.96	0.15	+	+
	787	71.4	370	1.04	1.83	5.97	-1.58	c_{cold}	***	0.92	0.2	+	+
	657	123	775	1.08	-0.35	6.53	-2.37	b_x	***	0.79	0.23	+	+
	1774	95.9	420	2.07	7.76	-6.21	-0.36	c_{heat}	NS	0.41	0.48	+	+
	715	116	520	2.08	0.60	-7.86	-0.66	c_{heat}	NS	0.22	0.5	+	+
	786	16.2	43	3.01	-4.98	-7.46	2.58	c_{cold}	***	0.04	0.62	+	+
	944	143	801	3.09	4.10	6.78	-1.62	c_{cold}	***	0.86	0.25	+	+
	47	38.7	179	4.03	2.73	-4.07	7.14	b_x	**	0	0.52	+	+
	93	46	212	4.04	3.86	-8.24	3.04	b_x	**	0	0.52	+	+
	123413	59.7 19.9	277 77	4.05 5.01	12.3 -2.69	8.30 -	0.11 -	a_{cold} b_{opt}	*** NS	0.93 0.28	0.13 0.5	- +	+ +

					7.32	2.13						
222	37.9	148	5.01	2.13	-7.76	0.63	b_x	***	0.1	0.59	+	+
344	44.3	169	5.01	-3.97	-10.6	-2.56	b_{opt}	***	0.05	0.58	+	+
1437	63.9	245	5.03	1.01	8.24	2.22	b_{opt}	***	0.65	0.13	+	+
313	67	264	5.03	-11.0	-12.7	-7.59	b_{opt}	***	0	0.62	+	+
1206	71.5	291	5.03	-2.02	-11.4	-5.04	b_{opt}	***	0	0.54	+	+
174	72.3	296	5.03	-0.59	9.90	3.30	c_{heat}	*	0.5	0.12	+	+
973	84.5	370	5.04	-0.41	-9.01	0.52	c_{cold}	***	0	0.59	+	+
538	86	376	5.04	-1.05	-8.89	1.35	c_{cold}	NS	0.3	0.5	+	+
953	90.3	394	5.05	-1.34	-5.32	3.06	c_{cold}	***	0.08	0.76	+	+
546	53.9	230	7.02	-6.64	-9.10	-2.19	b_{opt}	***	0.11	0.78	+	+
1274	55.5	248	7.02	-6.10	-9.37	-2.62	b_{opt}	***	0.11	0.75	+	+
544	55.8	251	7.02	25.7	12.7	7.62	a_{cold}	***	0.93	0.13	-	+
280	58.7	197	8.03	2.45	8.92	-1.00	c_{cold}	***	1	0.23	+	+
24	81.7	355	8.05	-11.4	4.31	-4.88	b_x	*	0.52	0.13	+	+
1162	77.7	304	9.04	-3.57	-10.8	-2.93	b_{opt}	***	0	0.63	+	+
754	60.3	278	10.04	3.35	-5.82	3.28	b_x	***	0.04	0.65	+	+
756	60.4	279	10.04	6.19	-3.15	6.34	b_x	**	0.17	0.6	+	+

279	60.5	280	10.04	-5.31	-8.67	-0.93	b_{opt}	***	0.08	0.61	+	+
1119	62.5	297	10.04	-2.07	6.53	-0.24	b_x	***	0.71	0.21	+	+
474	63.5	306	10.04	-8.38	3.24	-5.83	b_x	**	0.66	0.24	+	+
11	NA	NA	NA	11.3	-4.04	4.48	b_x	**	0	0.54	+	+
18	NA	NA	NA	9.69	9.80	3.65	b_{opt}	NS	0.52	0.27	+	+
164	NA	NA	NA	-2.92	5.46	-1.59	b_x	***	0.74	0.06	+	+
287	NA	NA	NA	-3.93	-4.53	5.12	c_{cold}	***	0.06	0.73	+	+
438	NA	NA	NA	-28.9	-14.2	-8.63	a_{cold}	***	0.03	0.82	-	+
737	NA	NA	NA	-16.9	-13.9	-8.19	a_{cold}	***	0	0.58	-	+
755	NA	NA	NA	27.5	12.9	7.24	a_{cold}	***	1	0.13	-	+
927	NA	NA	NA	-22.1	-15.4	-8.90	a_{cold}	***	0	0.57	-	+
985	NA	NA	NA	2.26	10.4	2.51	b_{opt}	***	0.55	0	+	+
1041	NA	NA	NA	-3.27	-10.4	-3.25	b_{opt}	***	0	0.59	+	+
1429	NA	NA	NA	0.90	-7.49	2.32	b_x	***	0.09	0.75	+	+
1471	NA	NA	NA	1.04	-7.94	-2.90	c_{heat}	NS	0.42	0.49	+	+
1472	NA	NA	NA	-4.28	6.84	1.42	c_{heat}	NS	0.49	0.41	+	+
1623	NA	NA	NA	6.95	-5.71	4.38	b_x	***	0	0.54	+	+
1758	NA	NA	NA	13.2	-4.84	5.08	b_x	***	0	0.59	+	+

	1818	NA	NA	NA	10.9	-5.44	3.54	b_x	***	0.11	0.61	+	+
	20	NA	NA	NA	-0.83	6.99	0.74	c_{heat}	**	0.55	0.11	+	+
	625	NA	NA	NA	-14.0	-13.1	-4.74	a_{cold}	***	0.05	0.6	-	+
L_{Ax}	1511	137	611	2.09	-0.13	0.96	-0.83	b_x	***	0.91	0.06	+	+
	756	60.4	279	10.04	0.21	-1.76	0.51	b_x	**	0.17	0.6	+	+
D_{Ax}	1177	58.4	275	3.04	0.91	2.75	-2.42	c_{cold}	**	1	0.36	+	+
D_{Lat}	804	105	504	9.06	1.56	0.71	-1.02	a_x	***	1	0.25	-	+
DW_{Rt}	1138	69.8	360	1.04	0.536	-0.28	0.524	b_x	**	0.19	0.56	+	+
	955	69.9	360	1.04	1.089	0.091	0.727	b_{ex}	***	0	0.54	+	+
	642	133	642	9.07	0.494	-0.39	0.086	b_x	***	0.12	0.7	+	+
	1638	NA	NA	NA	0.705	-0.59	-0.42	c_{heat}	*	0	0.44	+	+
DW_{RtSt}	151	83.8	370	8.05	2.87	-3.87	8.71	b_x	***	0	0.6	+	+
	1584	NA	NA	NA	-0.46	-5.03	15.3	c_{cold}	*	0.08	0.52	+	+
k_{Lat}/ER_{Ax}	31	63.2	316	1.04	0.74	9.96	-1.57	c_{cold}	***	0	0.57	-	-
	7	101	608	1.07	12.9	-7.91	6.18	b_x	NS	0	0.47	+	+
	1774	95.9	420	2.07	-3.72	10.8	-0.44	b_x	NS	0.41	0.48	-	-
	581	105	468	2.07	6.70	-	4.39	b_x	*	0.62	0.31	-	-

					8.07							
1511	137	611	2.09	4.02	-4.38	8.10	b_x	***	0.91	0.06	-	-
2	143	637	2.09	0.21	-4.85	5.38	b_x	***	1	0.18	-	-
726	8.9	4	3.0	-5.46	10.2	-4.11	b_x	***	0	0.67	-	-
786	16.2	43	3.01	-0.26	11.6	-5.17	b_x	***	0.04	0.62	-	-
47	38.7	179	4.03	-6.67	8.08	-7.82	b_x	**	0	0.52	-	-
93	46	212	4.04	-5.66	11.5	-6.08	b_x	**	0	0.52	-	-
13	19.9	77	5.01	-2.51	9.30	-0.75	b_x	NS	0.28	0.5	-	-
336	59.5	281	7.02	-0.02	9.81	-3.89	b_x	NS	0.33	0.47	-	-
24	81.7	355	8.05	4.85	-6.65	5.28	b_x	*	0.52	0.13	-	-
1162	77.7	304	9.04	0.56	13.4	-0.78	c_{cold}	***	0	0.63	-	-
754	60.3	278	10.04	-4.97	9.67	-6.03	b_x	***	0.04	0.65	-	-
756	60.4	279	10.04	-3.68	10.2	-7.43	b_x	**	0.17	0.6	-	-
279	60.5	280	10.04	0.07	12.1	-2.52	c_{cold}	***	0.08	0.61	-	-
11	NA	NA	NA	-5.11	8.49	-6.25	b_x	**	0	0.54	-	-
32	NA	NA	NA	1.04	-4.77	5.89	b_x	***	0.7	0.26	-	-
287	NA	NA	NA	5.15	10.8	-	c_{cold}	***	0.06	0.73	-	-

						2.73						
1002	NA	NA	NA	-1.71	7.98	-2.81	b_x	***	0.07	0.73	-	-
1041	NA	NA	NA	-4.78	10.6	-1.42	b_x	***	0	0.59	-	-
1273	NA	NA	NA	-7.65	12.6	-7.10	b_x	NS	0.14	0.46	-	-
1430	NA	NA	NA	-0.77	-13.6	3.93	c_{cold}	NS	0.65	0.36	-	-
1471	NA	NA	NA	-2.23	12.7	-0.05	b_x	NS	0.41	0.49	-	-
1472	NA	NA	NA	1.47	-11.7	0.14	b_x	NS	0.49	0.41	-	-
1818	NA	NA	NA	-6.80	9.02	-5.17	b_x	***	0.11	0.61	-	-
20	NA	NA	NA	8.44	-4.55	3.14	b_x	**	0.55	0.11	-	-

*, **, ***, NS indicate significance level of P <0.05, <0.01, <0.001 and not significant, respectively, based on a χ^2 two sample test for allele distribution between the heterotic groups.

NA: Marker is not yet mapped to one of the 10 chromosomes on the Keygene integrated map.